Carbon 146 (2019) 320–328

Contents lists available at ScienceDirect

Carbon

journal homepage: www.elsevier.com/locate/carbon

Review article

Graphene oxide based materials for desalination

Xiuqiang Li, Bin Zhu, Jia Zhu*

National Laboratory of Solid State Microstructures and College of Engineering and Applied Sciences, Nanjing University, Nanjing, 210093, China

ARTICLE INFO

Article history:
Received 17 October 2018
Received in revised form
26 January 2019
Accepted 3 February 2019
Available online 6 February 2019

Keywords:
Graphene oxide
Desalination
Solar evaporation
Filtration

ABSTRACT

Nowadays, water shortage has become an ever-increasing severe problem for human beings. Lately, there has been exciting progress in two different ways for desalination, namely, interfacial solar evaporation and film filtration. Graphene oxide based film is playing a critical role in both developments due to its high absorption, porous structure, high chemical stability, hydrophilicity, and excellent anti-fouling properties. In this works, we first introduce the mechanisms and key requirements for interfacial solar evaporation and filtration based desalination, and then explain how various forms of graphene oxide can be tailored for both types of desalination. Then, we summarize and discuss recent researches concerning both relevant technology advances and persisting problems, and finally provide a prospective view.

Contents

1. Introduction

Currently, about 4 billion people in the world suffer from severe water shortage for at least one month of each year [1]. About 97.5% of all water on the earth is seawater, therefore seawater desalination is regarded as one of most promising technologies to alleviate

* Corresponding author.
E-mail address: jiazhu@nju.edu.cn (J. Zhu).

https://doi.org/10.1016/j.carbon.2019.02.007
0008-6223/

water shortage. In the past few years, several technologies for desalination such as solar evaporation and filtration have progressed rapidly [2–4]. Graphene oxide (GO), among various forms of nanomaterials, provides tremendous opportunities for rational design and tailoring for solar evaporation and film filtration because of its high absorption, porous structure, high chemical stability, hydrophilicity, and excellent anti-fouling properties [3,4]. Nowadays, GO has widely been used as absorber in solar desalination and as filtration film in desalination.

In this review, we focus on the recent progress of GO based desalination. First, we discussed the mechanisms and key requirements for GO based interfacial solar evaporation and filtration, and further explained how various forms of GO can be tailored for both types of desalination. Then, we summarized the recent researches concerning both relevant technological advances. At the end, we presented current challenges and crucial issues of recent GO based desalination, aiming to provide a guideline for further development of GO based desalination.

2. Mechanisms and features

2.1. GO based solar steam generation

As shown in Fig. 1a, during the interfacial solar evaporation, GO film can be an excellent absorber [5–23], taking in sunlight and converting it into thermal energy through optically excited electron-electron scattering, thus heating and evaporating water. The added benefit of GO films with nanochannels is that it provides a path for water supply and vapor escape. Desalination is therefore achieved by the phase-changing process, with the non-volatile ions left. Finally, fresh water is collected through condensation. This technology has several main features: (1) it is exclusively driven by solar energy; (2) it exhibits extremely high ion removal efficiency; (3) it requires low capital investment. All of these make this technology highly applicable as a portable device that can be used in developing countries and remote areas that lack infrastructure.

2.2. GO based filtration film

As shown in Fig. 1b, GO nanosheets can be assembled as stacked GO films with 2D nanochannels between two adjacent GO nanosheets for desalination [24–51]. The d-spacing of nanochannels is about 0.76 nm (Dry GO, Note: this value can be tuned and will be discussed in more details later), which is larger than water molecules (0.275 nm) so as to enable the permeation of water. On the contrary, the ions (Li^+ (0.764 nm), Na^+ (0.716 nm), K^+ (0.662 nm), Mg^{2+} (0.856 nm), Ca^{2+} (0.824 nm), F^- (0. 704 nm), Cl^- (0.664 nm), Br^- (0.660 nm)) [52] can be separated from seawater through size exclusion and electrostatic interactions, thus achieving desalination via GO film filtration. There are several main features about this technology: (1) it exhibits high water flux; (2) it requires relatively high capital investment; and (3) it requires electricity power to drive. All of these features determine that this technology is particularly suitable for centralized solution.

3. GO based solar steam generation for desalination

During solar steam generation (as shown in Fig. 2), the solar energy is first absorbed and converted into heat energy by the absorber. Note: the electrons can be excited under solar irradiation in carbon-based materials, and then the excited electrons are quickly relaxed and generate heat by electron-electron scattering. Then, the heat energy heats up the surface water, resulting in evaporation. Usually, the absorber's temperature is higher than the ambient temperature, so it also brings heat losses (Heat losses via conduction, convection and radiation). The whole process can be expressed mathematically as:

$$mh_{fg} = A\alpha q_{solar} - A\varepsilon\sigma(T^4 - T_\infty 4) - Ah(T - T_\infty) - A\lambda dt / dx \quad (1)$$

where m is the mass change of the steam, h_{fg} is the latent heat of steam, A is the area of the absorber, α is the solar absorptance, q_{solar} is the solar energy density, ε is the emissivity of the material, σ is the Stefan - Boltzmann constant, T is the absorber temperature, T_∞ is the ambient temperature, h is the convection heat transfer coefficient, λ is the thermal conductivity of the material and dt/dx is the temperature gradient of the absorber. Obviously, in order to obtain high efficiency (more details will be discussed later on), optical and heat losses should be suppressed.

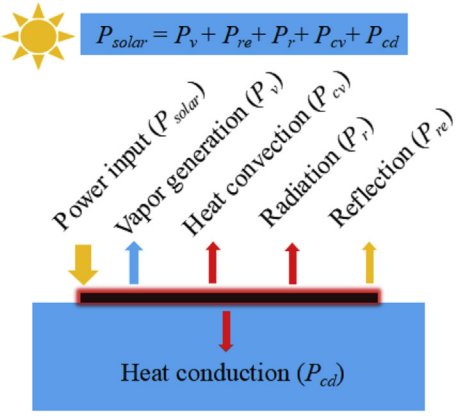

Fig. 2. The physical process of interfacial solar evaporation. (A colour version of this figure can be viewed online.)

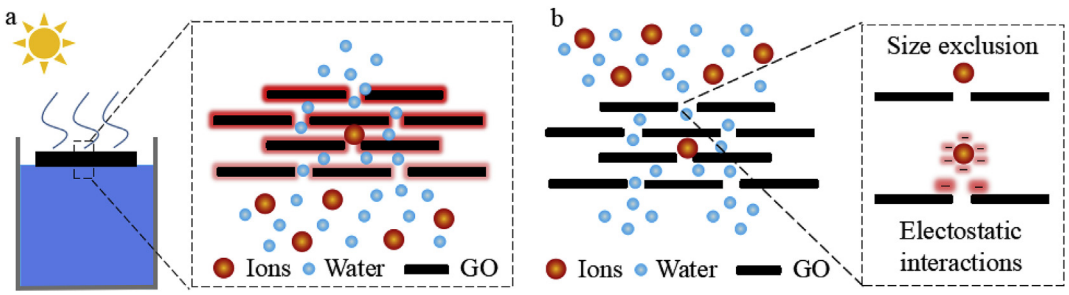

Fig. 1. (a) Schematic of GO film based interfacial solar evaporation for desalination. (b) Schematic of GO film based filtration for desalination. (A colour version of this figure can be viewed online.)

The energy conversion efficiency is defined as the ratio of the total enthalpy of water and the total energy of the sun to the absorber in the process of generating water vapor driven by the solar energy. The solar-to-steam conversion efficiency can be expressed as [5,53–55].

$$\eta = m(Lv + Q) / Pin \quad (2)$$

where $\dot{m}$ is the mass flux ($\dot{m} = m_{Light} - m_{Dark}$) kg m^{-2} h^{-1} (m_{Light} represents the mass change of water under solar irradiation and m_{Dark} represents the mass change of water without solar irradiation), Lv is the latent heat of vaporization of water ($Lv(T) = 1.91846 \times 106\ [T/(T - 33.91)]^2$ J kg^{-1}, where T is the temperature of vaporization) [27], Q is the sensible heat and P_{in} is the incident solar energy on the absorber surface.

3.1. Solar absorber (optical management)

As shown in equ. (1), efficient absorption is critical in highly efficient solar steam generation. Li et al. [6] has demonstrated a GO film (as shown in Fig. 3a) prepared by vacuum filtration can achieve >94% absorption (weighted by standard solar spectrum of air mass 1.5 global (AM1.5G)) from 250 to 2500 nm for efficient solar steam generation. Furthermore, the result also shows that the GO film has a porous structure, and that hydrophilicity is a suitable characteristic for absorbers in solar steam generation. Currently, some new GO based structures have been selected as absorbers like vertically aligned reduced GO (RGO) film (as shown in Fig. 3b and c) [7], 3D cross-linked polymer-like RGO material [8] (as shown in Fig. 3d) and RGO ball-based film [9] (as shown in Fig. 3e). Compared with the layer-by-layer structure obtained by vacuum filtration, the surface roughness of these films is increased while the optical reflection is decreased, which increases the absorption of the absorber (>97%) (as shown in Fig. 3f). Based on this, some mixed absorbers, such as GO/carbon nanotubes [10], GO/cellulose esters [11], etc. have also been selected as absorbers and they have achieved high absorption (>97%) (as shown in Fig. 3f). The absorption of GO film can also be enhanced by improving the reduction degree and hydrophilic property of GO film [12,13].

3.2. Heat management

As shown in equ. (1), apart from optical management, heat management (i.e. managing heat losses from conduction, convection and radiation) is also critical to highly efficient solar steam generation. GO films with low cross-plane thermal conductivity is beneficial for suppressing conduction loss. In order to further suppress conduction loss, various GO aerogel [14] and GO hybrid films [15,16] with low thermal conductivity have also been used. However, in application, even the low thermal conductivity of the GO based materials, water (which possesses a very high thermal conductivity ~ 0.6 W m^{-1} K^{-1}) will fill the GO based materials due to their porous structure and hydrophilicity, resulting in high thermal conductivity for the whole system. As a result, a significant portion of the absorbed energy is lost to the bulk water. Therefore, high solar-to-steam conversion efficiency (~80%) are mostly achieved with the aid of insulation containers or optical concentration techniques. For example, Jiang et al. [15] reported a bilayered biofoam composed of bacterial nanocellulose and RGO for solar steam generation (as shown in Fig. 4a and b). Even the thermal conductivity of this material in dry state is about 0.069 W m^{-1} K^{-1} at room temperature, the thermal conductivity is increased to about

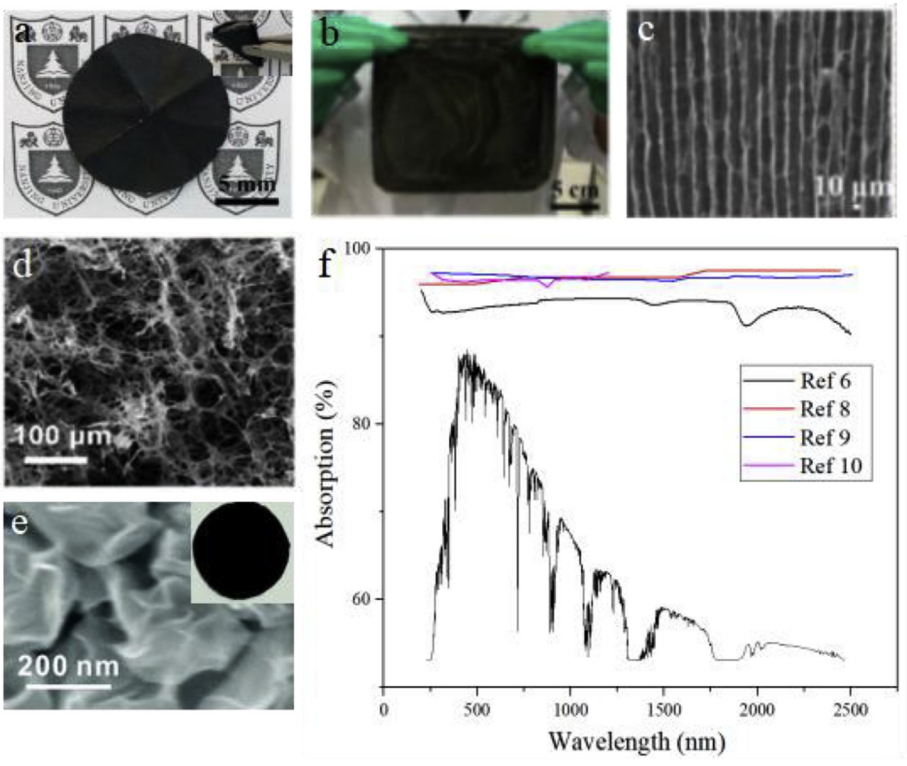

Fig. 3. (a) The optical image of folded GO film [6]. The optical image (b) and scanning electron microscope (SEM) (c) image of vertically aligned RGO film [7]. (d) The SEM image of 3D cross-linked polymer-like RGO material [8]. (e) The optical image and SEM image of RGO ball-based film [9]. (f) Measured light absorption performance of several representative GO based solar absorbers. (A colour version of this figure can be viewed online.)

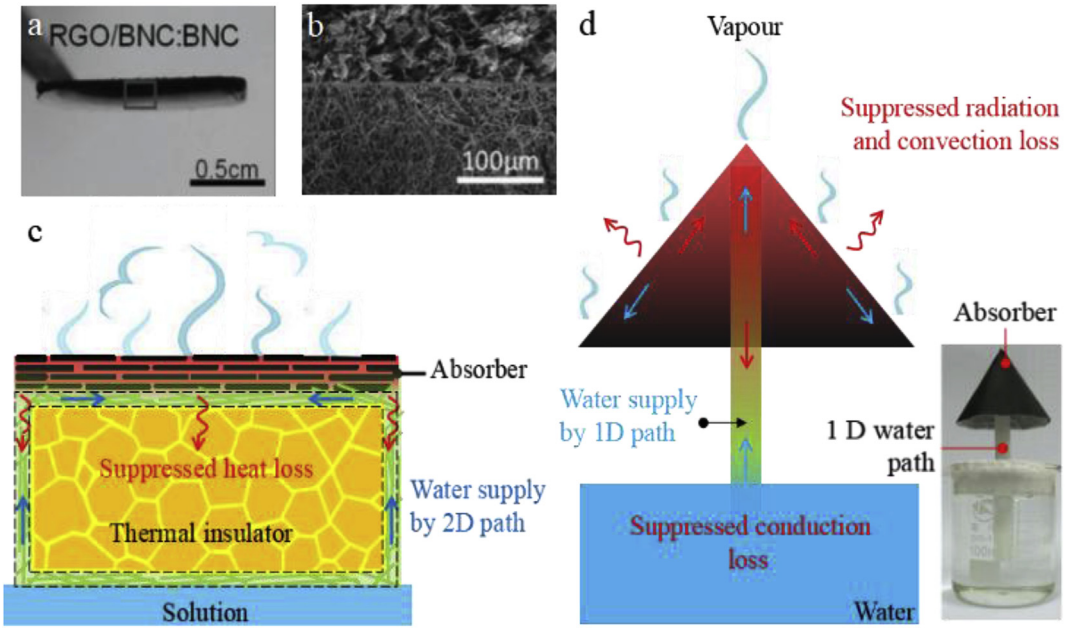

Fig. 4. Optical image (a) and SEM images of cross-section at the interface (b) of RGO/bacterial nanocellulose (BNC): BNC aerogel [15]. (c) Schematic of GO based solar desalination with 2D water path [6]. (d) Schematic and optical image of artificial transpiration device with 1D water path [5]. (A colour version of this figure can be viewed online.)

0.8 W m^{-1} K^{-1} in wet state. Therefore, ~83% solar-to-steam conversion efficiency can be achieved when the concentration techniques (10 kW m^{-2}) are used.

In order to overcome this challenge, it has been proposed that confining water into a one-dimensional (1D) water path (it means the water supply is just through a columnar, which are confined in other two dimensions) and two-dimensional (2D) water path (it means the water supply is just through a thin layer, which are confined in the third dimension) can decouple the water supply and thermal conduction. For example, as shown in Fig. 4c Li et al. [6] demonstrated that a GO film is not in direct contact with bulk water, but it is in indirect contact with the bulk water through a 2D water path, which is enabled by a thin layer of hydrophilic cellulose that is wrapped over the surface of the polystyrene foam. The water supply is pumped to the absorber by capillary force through hydrophilic cellulose while the conduction heat loss is suppressed by the hydrophobic polystyrene foam (thermal conductivity is about 0.04 W m^{-1} K^{-1}). Finally, 78% solar-to-steam conversion efficiency was achieved without any insulative container or optical concentration. Based on this strategy, higher efficiency (~83%) has been achieved through optimization of material structure and 2D water path [17].

After fixing the conduction loss problem, some research has shifted focus to methods of reducing convective and radiative heat loss. Currently, one efficient strategy is to reduce the temperature of evaporation. As shown in equ. (1), the convection loss and radiation loss is minimized when the temperature difference between the absorber and the ambient temperature is reduced. Currently, Li et al. [5] reported that three-dimensional artificial transpiration devices comprised of GO films have been proposed as they can increase effective evaporation area (as shown in Fig. 4d). As a result, the evaporation temperature can be significantly decreased. With the addition of this technique, 85% solar-to-steam conversion efficiency has been achieved without insulative containers or optical concentration.

3.3. Water supply

The water supply of absorber itself is also very important, especially for reduced GO film. For example, Fu et al. [12] reported the solar-to-vapor conversion efficiency can be increased by 15% through tuning the hydrophilic property of reduced GO film.

3.4. Purification effects

As mentioned above, high salt rejection rate is an advantageous property for solar desalination. In general, this technology can decrease the salinity of seawater by 3–4 orders of magnitude below the values obtained through film-based seawater desalination (10–500 mg L^{-1}) as well as the standard (200 mg L^{-1}) established by the World Health Organization (WHO). Furthermore, some works reported that the purification is almost completely independent on pH value, salt concentration and ion species due to high chemical stability of GO based materials [5,8]. For example, Li et al. [5] has designed a GO based absorber for interfacial solar desalination. The result shown that the collected water from the condensed vapor is pure enough to meet WHO drinking water standards, even though the different ion species, such as Cu^{2+}, Cd^{2+}, Pb^{2+} and Zn^{2+}, were used. Meanwhile, they also demonstrated the purification effect is almost the same at different pH conditions (pH = 2, 4 and 7).

3.5. Zero liquid discharge

Zero liquid discharge is also an advantageous property for solar steam generation. Finnerty et al. [18] has reported a nature-inspired leaf prepared by GO film, which can achieve zero liquid discharge and high performance (as shown in Fig. 5a). The works showed that with the aid of 1D water path, 78% conversion efficiency can be achieved, and so is the stable performance during a long-term evaporation experiment with a 15 wt % NaCl solution, even though the salt deposits on the GO film were severe (as shown in Fig. 5b). Furthermore, the GO leaf can be easily restored to its pristine performance by simply scraping off salt crystals from GO film surface and rinsing with water.

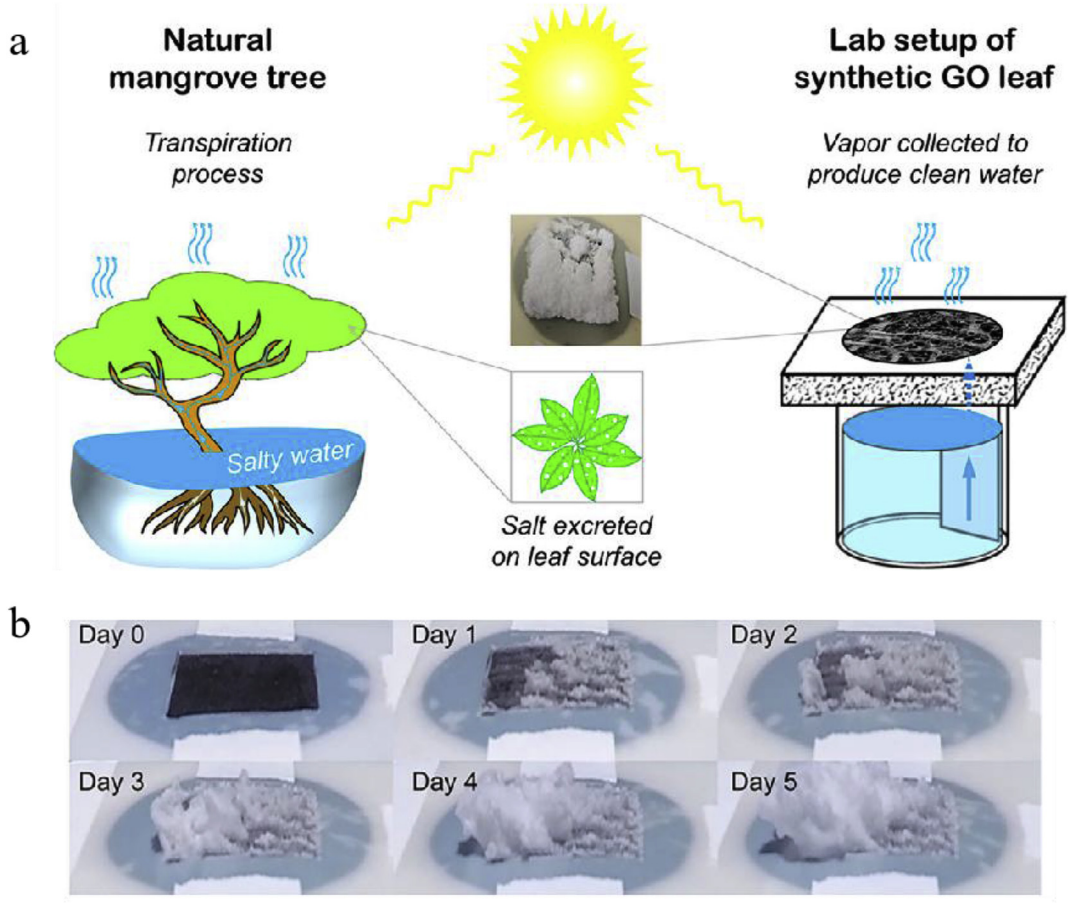

Fig. 5. (a) Tree inspired GO film based solar desalination device. (b) Time-lapse optical image of salt crystal formation on the GO leaf surface during a 5-day evaporation experiment using 15 wt % NaCl solution [18]. (A colour version of this figure can be viewed online.)

4. Filtration member based on GO for desalination

As mentioned, GO multi-layer films with aforementioned properties are favorable candidates for next-generation desalination films. Salt rejection and water flux are the main figure of merit. Unfortunately, there is almost always a trade-off between the two. However, this trade-off can be broken using intercalation, changing deposition method of GO film or utilizing electrostatic interaction between GO and ions. The salt rejection rate can be calculated by the feed and permeate concentrations using Eq. (3) as shown below [24,25]:

$$R(\%) = (Cf - Cp) / Cf \times 100\% \quad (3)$$

where R is the salt retention rate, and C_f and C_p are the feed and salt permeate concentrations (ppm). The permeation rate can be calculated at a certain pressure using Eq. (4) as shown below:

$$\text{Water flux} = Q / (A \times \Delta t) \quad (4)$$

where Q is the permeate quantity (L), A is the area of film (m^2), and Δt is the processing time.

4.1. Tuning of salt rejection rate and water flux of GO film

4.1.1. Intercalation of GO film for tuning salt rejection rate and water flux

Intercalation is an effective way to tune the salt rejection rate and water flux. Polymer intercalation is a frequently used strategy for tuning the salt rejection rate and water flux. So far, N-isopropylacrylamide-co-N, N′-methylene-bisacrylamide (0.48 nm) [26], polydopamine (0.345 nm) [27], 1, 4-phenylene diisocyanate [25], polyimide hollow fiber [28], 1, 4-cyclohyxanediamine and p-phenylenediamine (pPDA) (0.56 nm) [29] have all been selected as intercalated materials. For example, the chemical reduction of GO (RGO) laminates and a hydrophilic adhesive polydopamine layer were applied. RGO laminates sustainably retained their compacted nanochannels (0.345 nm) compared to pristine GO laminates, which increased the selectivity of hydrated ions. Moreover, the water absorption speed can be accelerated via improving the hydrophilicity of the RGO laminate surface by adding a polydopamine coating onto the RGO laminates. As a result of these synergistic effects, these hybrid films achieved an outstanding water flux of 36.6 L m^{-2} h^{-1}, and a high salt rejection rate of 92.0% [27].

Intercalation of other 2D materials (such as a few layers of graphene [30], monolayer titania [31], etc) is also usually helpful for tuning the salt rejection rate and water flux. For example, by intercalating monolayer titania (TO) nanosheets into GO film with mild ultraviolet reduction, the hybrid RGO/TO film showed excellent desalination performance. The result showed that the salt rejection rate can reach as high as 95% and water transfilm permeation can be retained at about 60%. Here, the decrease of d-spacing caused by photoreduction of the GO by TO under mild ultraviolet irradiation gave rise to the high salt rejection rate. The photoinduced hydrophilic transformation of the TO nanosheets within the GO film resulted in the preservation of the relatively

high water flux [30].

Ion intercalation is also an effective way to tune the d-spacing of GO films. Chen et al. [32] found that some cationic ions such as K^+, Na^+, Ca^{2+}, Li^+ or Mg^{2+} ions can tune the d-spacing of GO films with ångström precision. Moreover, GO films (as shown in Fig. 6a and b) can effectively reject other cations with larger hydrated volume when the GO film was inserted by a certain type of cation (as shown in Fig. 6c and d). The result showed that untreated GO films demonstrated Na^+, Mg^{2+} and Ca^{2+} permeation rates of 0.190 mol m^{-2} h^{-1}, 0.025 mol m^{-2} h^{-1} and 0.019 mol m^{-2} h^{-1}, respectively. For comparison, KCl-treated GO films showed the permeation rates of Na^+, Mg^{2+} and Ca^{2+} were below that of the cation detection limits. At the same time, the water flux of KCl-treated GO films can reach 0.36 L m^{-2} h^{-1}. The foundational mechanism revealed by first-principles calculations and ultraviolet absorption spectroscopy is that the location of the most stable cation adsorption is in functional groups and aromatic rings. Also, other cations such as Fe^{2+}, Co^{2+}, Cu^{2+}, Cd^{2+}, Cr^{2+} and Pb^{2+} are expected to be able to tune the d-spacing of GO films because they have much stronger interactions with graphene than Na^+. Apart from d-space tuning, Aaron et al. [30] demonstrated that the Ca^{2+} ion interaction with GO films (at present of deoxycholate) can improve salt rejection rates because these compounds of Ca^{2+} and deoxycholate confer zwitterionic behaviour to GO films.

4.1.2. Modification of GO film for tuning salt rejection rate and water flux

Apart from intercalation strategy, the preparation of GO film can also efficiently tune the salt rejection rate and water flux. Lately, Xu et al. [33] demonstrated that the ion selectivity and water flux can be synergetically regulated by controlling the deposition rate. The results showed that the GO films obtained by slow deposition not only can improve salt rejection rate, but also can obtain 2.5–4 times higher water flux than fast deposition. This is because the slow assembly contains both an oxidized surface facing another oxidized surface (O – O) and a pristine surface facing another pristine surface (P – P) subdomains and the fast assembly contains only an oxidized surface facing a pristine surface (O – P) subdomains (as shown in Fig. 7a). The simulation study showed that the water transport in nanochannels with the O – O and O – P subdomains is slower than hydrophobic nanochannels with the P – P subdomains. The corresponding water flux and salt rejection can be found in Fig. 7b and c. This exciting finding provides a new approach for synergetic regulation of ion selectivity and water flux. However, the method's reliability and molecular-sieving preciseness still need to be further explored.

Preparation of the nanochannels is also an efficient way to tune salt rejection rate and water flux. Huang et al. [34] reported an ultrafiltration nanostrand-channelled GO (NSC-GO) film with numerous nanochannels with diameters ranging from 3 to 5 nm. These films were prepared via the deposition of a mixed solution of copper hydroxide nanostrands and GO sheets onto a porous support, followed by hydrazine reduction, and finalized by removing the copper hydroxide nanostrands. Without compromising the salt rejection rate, this technique resulted in a water flux of 695 ± 20 L m^{-2} h^{-1} bar^{-1}, 10x higher than untreated GO film and 100x higher than commercial ultrafiltration films with a similar salt rejection rate. The salt rejection rate of all the negatively charged molecules is dominated by the molecular-sieving mechanism while the high water flux can be attributed to both significantly enhanced

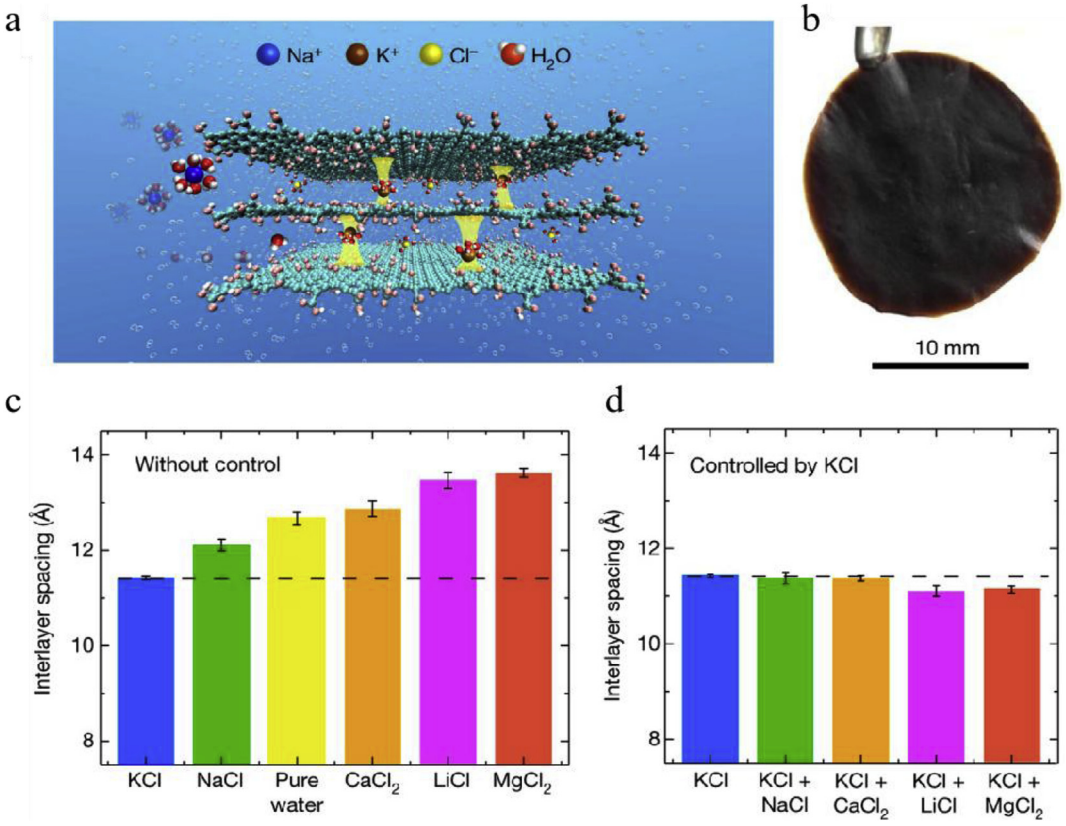

Fig. 6. (a) A schematic of GO film with different ions and water molecules. Yellow pillars between the GO sheets depict the fixation of interlayer spacing by hydrated K^+. (b) Optical image of a freestanding GO film prepared by drop-casting of a 5 mg ml^{-1} GO suspension. (c) d-spacings of GO film immersed in pure water or in various 0.25 mol l^{-1}salt solutions. (d) d-spacings of GO film that were soaked in KCl solution, followed by immersion in various salt solutions [32]. (A colour version of this figure can be viewed online.)

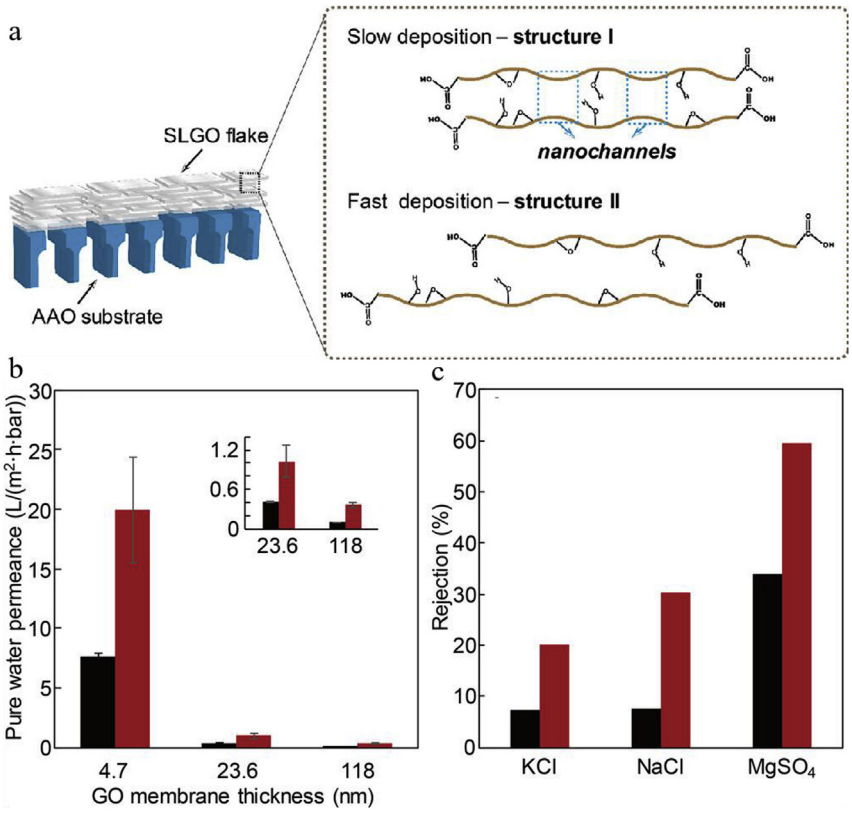

Fig. 7. (a) The schematic of structure of GO film prepared by slow deposition and fast deposition. (b) Water permeation through GO film prepared by fast (black) and slow-deposition (red) rates. (c) Salt rejection of 4.7 nm thick GO film prepared at fast/slow deposition rate [33]. (A colour version of this figure can be viewed online.)

porosity and decreased channel length of several micrometres in the NSC- GO film.

Some techniques based on the modification of GO films have been selected to tune salt rejection rate and water flux. For example, Han et al. [35] demonstrated around a 20–60% salt rejection rate at 21.8 L m^{-2} h^{-1} bar^{-1} by tuning a functional group of GO and utilizing electrostatic interactions. Recently, Hong et al. [36] demonstrated that ion rejection in GO films were influenced by the nanochannel's surface charge. These surface charges enabled the GO films to achieve a 96% salt rejection rate. Therefore, increasing the film's surface charge can also improve the salt rejection rate in GO films without sacrificing the water flux.

4.1.3. Other methods for tuning salt rejection rate and water flux

Encapsulation is another efficient method to tune the d-spacing of GO films. Abraham et al. [37] recently discovered an effective way of controlling the d-spacing in GO films in the sub nanometer range. The GO films with desirable d-spacing were encapsulated and stacked together using stycast epoxy, which added energy barriers for swelling while also enabling accurate and tunable ion sieving capabilities. This method resulted in a salt rejection rate of 97% for NaCl with a water flux of about 0.5 L m^{-2} h^{-1}.

4.2. Tuning of stability of GO film

The d-spacing in GO films is the critical parameter that determines the desalination property. Swelling of GO film always increases the d-spacing of GO films. Recently, Zheng et al. [38] reported the max d-spacing of GO film in water can reach as long as 6–7 nm at equilibrium after swelling. The oxygenated functional groups in the GO makes it very hydrophilic, resulting in a tendency for the materials to absorb water and swell. There are some strategies (such as reduction, mixing with polyer, encapsulation, etc) to resolve this issue. For example, Abraham et al. [37] showed that it is possible to mitigate the swelling of GO film in water simply by incorporating graphene plates into GO film. The composites referring as GO–graphene film exhibit notably less swelling (difference in d-spacing of ≈4 Å) as compared to standard GO film. The observed huge difference in d-spacing between GO film and GO-graphene film can be attributed to graphene's hydrophobicity that limits the water intake. Although some techniques can help mitigate the swelling, the effectiveness of these techniques in long-time cycle or prolonged use need to be further researched.

"One thing that need more attention is the symmetry of GO film [3]. Tang et al. [39] found that the chemical structure of reduced GO film out of the vacuum-filtrated method is asymmetric, which should be carefully considered for applications of desalination. "

5. Conclusions and outlook

In summary, GO with high absorption, porous structure, high chemical stability, hydrophilicity, and excellent anti-fouling properties has been proved to be a promising material for desalination through interfacial solar evaporation and filtration. Currently, although some progress has been made, there are still a few key issues upon which we lack adequate understanding.

For interfacial solar evaporation based approach, (1) it is necessary to further explore the influence of intrinsic properties of GO film on the process of solar evaporation and desalination. (2) Salt precipitation tends to destroy the water path or micro structure of GO film that causes the decrease of efficiency. Therefore, salt rejection is a very important issue to solar desalination. Even

though some researchers have achieved NaCl rejection through concentrated diffusion, the complete rejection of ions like Ca^{2+} and Mg^{2+} has yet to be accomplished because their concentrations approach saturation in seawater; (3) More work need to be done to explore the stability of GO film so as to accelerate the application of GO film; For filtration based approach, (1) it is critical to probe fundamentally how the intrinsic properties of GO can influence the filtration process; (2) the swelling of GO film in water has an adverse effect on the rejection of salt and thus it is crucial we learn to better mitigate it for desalination; (3) reaching an 100% salt rejection rate is a tough task for GO films. While the methods discovered until today have achieved unprecedented effect, it is important that the scientific community continues searching new strategies to achieve a higher salt rejection rate and larger water flux by improving the designs of functional group and micro structure of GO films.

Acknowledgments

We acknowledge the micro-fabrication center of National Laboratory of Solid State Microstructures (NLSSM) for technique support. This work is jointly supported by the State Key Program for Basic Research of China (No. 2015CB659300), the National Key Research and Development Program of China (No. 2017YFA0205700), National Natural Science Foundation of China (Nos. 11621091, 11574143, 61735008), and the Fundamental Research Funds for the Central Universities (Nos. 021314380135, 021314380128).

References

[1] M.M. Mekonnen, A.Y. Hoekstra, Four billion people facing severe water scarcity, Sci. Adv. 2 (2016), e1500323.
[2] P. Wang, Emerging investigator series: the rise of nano-enabled photothermal materials for water evaporation and clean water production by sunlight, Environ. Sci.: Nano 5 (5) (2018) 1078–1089.
[3] S. Homaeigohar, M. Elbahri, Graphene membranes for water desalination, NPG Asia Mater. 9 (8) (2017) e427.
[4] J.R. Werber, C.O. Osuji, M. Elimelech, Materials for next-generation desalination and water purification membranes, Nat. Rev. Mater. 1 (5) (2016) 16018.
[5] X. Li, R. Lin, G. Ni, N. Xu, X. Hu, B. Zhu, G. Lv, J. Li, S. Zhu, J. Zhu, Three-dimensional artificial transpiration for efficient solar waste-water treatment, Natl. Sci. Rev. 5 (1) (2018) 70–77.
[6] X. Li, W. Xu, M. Tang, L. Zhou, B. Zhu, S. Zhu, J. Zhu, Graphene oxide-based efficient and scalable solar desalination under one sun with a confined 2D water path, Proc. Natl. Acad. Sci. U. S. A. 113 (49) (2016) 13953–13958.
[7] P. Zhang, J. Li, L. Lv, Y. Zhao, L. Qu, Vertically aligned graphene sheets membrane for highly efficient solar thermal generation of clean water, ACS Nano 11 (5) (2017) 5087–5093.
[8] Y. Yang, R. Zhao, T. Zhang, K. Zhao, P. Xiao, Y. Ma, P.M. Ajayan, G. Shi, Y. Chen, Graphene-based standalone solar energy converter for water desalination and purification, ACS Nano 12 (1) (2018) 829–835.
[9] W. Hao, K. Chiou, Y.M. Qiao, Y.M. Liu, C.Y. Song, T. Deng, J.X. Huang, Crumpled graphene ball-based broadband solar absorbers, Nanoscale 10 (2018) 6306–6312.
[10] Y. Li, T. Gao, Z. Yang, C. Chen, W. Luo, J. Song, E. Hitz, C. Jia, Y. Zhou, B. Liu, B. Yang, L. Hu, 3D-printed, all-in-one evaporator for high-efficiency solar steam generation under 1 sun illumination, Adv. Mater. 29 (26) (2017) 1700981.
[11] G. Wang, Y. Fu, X. Ma, W. Pi, D. Liu, X. Wang, Reusable reduced graphene oxide based double-layer system modified by polyethylenimine for solar steam generation, Carbon 114 (2017) 117–124.
[12] Y. Fu, G. Wang, X. Ming, X.H. Liu, B.F. Hou, T. Mei, J.H. Li, J.Y. Wang, X.B. Wang, Oxygen plasma treated graphene aerogel as a solar absorber for rapid and efficient solar steam generation, Carbon 130 (2018) 250–256.
[13] A.K. Guo, X. Ming, Y. Fu, G. Wang, X.B. Wang, Fiber-based, double-sided, reduced graphene oxide films for efficient solar vapor generation, ACS Appl. Mater. Interfaces 9 (2017) 29958–29964.
[14] X.Z. Hu, W.C. Xu, L. Zhou, Y.L. Tan, Y. Wang, S.N. Zhu, J. Zhu, Tailoring graphene oxide-based aerogels for efficient solar steam generation under one sun, Adv. Mater. 29 (2017) 1604031.
[15] Q.S. Jiang, L.M. Tian, K.K. Liu, S. Tadepalli, R. Raliya, P. Biswas, R.R. Naik, S. Singamaneni, Bilayered biofoam for highly efficient solar steam generation, Adv. Mater. 28 (2016) 9400–9407.
[16] G. Wang, Y. Fu, A.K. Guo, T. Mei, J.Y. Wang, J.H. Li, X.B. Wang, Reduced graphene oxide-polyurethane nanocomposite foam as a reusable photoreceiver for efficient solar steam generation, Chem. Mater. 29 (2017) 5629–5635.
[17] L. Shi, Y.C. Wang, L.B. Zhang, P. Wang, Rational design of a bi-layered reduced graphene oxide film on polystyrene foam for solar-driven interfacial water evaporation, J. Mater. Chem. A 5 (2017) 16212–16219.
[18] C. Finnerty, L. Zhang, D.L. Sedlak, K.L. Nelson, B. Mi, Synthetic graphene oxide leaf for solar desalination with zero liquid discharge, Environ. Sci. Technol. 51 (20) (2017) 11701–11709.
[19] V. Kashyap, A. Al-Bayati, S.M. Sajadi, P. Irajizad, S.H. Wang, H. Ghasemi, A flexible anti-clogging graphite film for scalable solar desalination by heat localization, J. Mater. Chem. A 5 (29) (2017) 15227–15234.
[20] X. Li, J. Li, J. Lu, N. Xu, C. Chen, X. Min, B. Zhu, H. Li, L. Zhou, S. Zhu, T. Zhang, J. Zhu, Enhancement of interfacial solar vapor generation by environmental energy, Joule 2 (7) (2018) 1331–1338.
[21] Y. Li, T. Gao, Z. Yang, C. Chen, Y. Kuang, J. Song, C. Jia, E.M. Hitz, B. Yang, L. Hu, Graphene oxide-based evaporator with one-dimensional water transport enabling high-efficiency solar desalination, Nano Energy 41 (2017) 201–209.
[22] K.K. Liu, Q. Jiang, S. Tadepalli, R. Raliya, P. Biswas, R.R. Naik, S. Singamaneni, Wood-graphene oxide composite for highly efficient solar steam generation and desalination, ACS Appl. Mater. Interfaces 9 (8) (2017) 7675–7681.
[23] J. Yang, Y. Pang, W. Huang, S.K. Shaw, J. Schiffbauer, M.A. Pillers, X. Mu, S. Luo, T. Zhang, Y. Huang, G. Li, S. Ptasinska, M. Lieberman, T. Luo, Functionalized graphene enables highly efficient solar thermal steam generation, ACS Nano 11 (6) (2017) 5510–5518.
[24] Y. Shi, C. Li, D. He, L. Shen, N. Bao, Preparation of graphene oxide–cellulose acetate nanocomposite membrane for high-flux desalination, J. Mater. Sci. 52 (22) (2017) 13296–13306.
[25] B. Feng, K. Xu, A. Huang, Covalent synthesis of three-dimensional graphene oxide framework (GOF) membrane for seawater desalination, Desalination 394 (2016) 123–130.
[26] S. Kim, X. Lin, R. Ou, H. Liu, X. Zhang, G.P. Simon, C.D. Easton, H. Wang, Highly crosslinked, chlorine tolerant polymer network entwined graphene oxide membrane for water desalination, J. Mater. Chem. A 5 (4) (2017) 1533–1540.
[27] E. Yang, C.-M. Kim, J.-h. Song, H. Ki, M.-H. Ham, I.S. Kim, Enhanced desalination performance of forward osmosis membranes based on reduced graphene oxide laminates coated with hydrophilic polydopamine, Carbon 117 (2017) 293–300.
[28] A. Huang, B. Feng, Synthesis of novel graphene oxide-polyimide hollow fiber membranes for seawater desalination, J. Membr. Sci. 548 (2018) 59–65.
[29] Y. Qian, C. Zhou, A. Huang, Cross-linking modification with diamine monomers to enhance desalination performance of graphene oxide membranes, Carbon 136 (2018) 28–37.
[30] A. Morelos-Gomez, R. Cruz-Silva, H. Muramatsu, J. Ortiz-Medina, T. Araki, T. Fukuyo, S. Tejima, K. Takeuchi, T. Hayashi, M. Terrones, M. Endo, Effective NaCl and dye rejection of hybrid graphene oxide/graphene layered membranes, Nat. Nanotechnol. 12 (11) (2017) 1083–1088.
[31] P. Sun, Q. Chen, X. Li, H. Liu, K. Wang, M. Zhong, J. Wei, D. Wu, R. Ma, T. Sasaki, H. Zhu, Highly efficient quasi-static water desalination using monolayer graphene oxide/titania hybrid laminates, NPG Asia Mater. 7 (2) (2015) e162-e162.
[32] L. Chen, G. Shi, J. Shen, B. Peng, B. Zhang, Y. Wang, F. Bian, J. Wang, D. Li, Z. Qian, G. Xu, G. Liu, J. Zeng, L. Zhang, Y. Yang, G. Zhou, M. Wu, W. Jin, J. Li, H. Fang, Ion sieving in graphene oxide membranes via cationic control of interlayer spacing, Nature 550 (7676) (2017) 380–383.
[33] W.L. Xu, C. Fang, F. Zhou, Z. Song, Q. Liu, R. Qiao, M. Yu, Self-Assembly: a facile way of forming ultrathin, high-performance graphene oxide membranes for water purification, Nano Lett. 17 (5) (2017) 2928–2933.
[34] H. Huang, Z. Song, N. Wei, L. Shi, Y. Mao, Y. Ying, L. Sun, Z. Xu, X. Peng, Ultrafast viscous water flow through nanostrand-channelled graphene oxide membranes, Nat. Commun. 4 (2013) 2979.
[35] Y. Han, Z. Xu, C. Gao, Ultrathin graphene nanofiltration membrane for water purification, Adv. Funct. Mater. 23 (29) (2013) 3693–3700.
[36] S. Hong, C. Constans, M.V.S. Martins, Y.C. Seow, J.A.G. Carrió, S. Garaj, Scalable graphene-based membranes for ionic sieving with ultrahigh charge selectivity, Nano Lett. 17 (2017) 728–732.
[37] J. Abraham, K.S. Vasu, C.D. Williams, K. Gopinadhan, Y. Su, C.T. Cherian, J. Dix, E. Prestat, S.J. Haigh, I.V. Grigorieva, P. Carbone, A.K. Geim, R.R. Nair, Tunable sieving of ions using graphene oxide membranes, Nat. Nanotechnol. 12 (6) (2017) 546–550.
[38] S. Zheng, Q. Tu, J.J. Urban, S. Li, B. Mi, Swelling of graphene oxide membranes in aqueous solution: characterization of interlayer spacing and insight into water transport mechanisms, ACS Nano 11 (6) (2017) 6440–6450.
[39] B. Tang, L.b. Zhang, R.Y. Li, J.B. Wu, M.N. Hedhilib, P. Wang, Are vacuum-filtrated reduced graphene oxide membranes symmetric? Nanoscale 8 (2016) 1108–1116.
[40] B.X. Min, Graphene oxide membranes for ionic and molecular sieving, Science 343 (2014) 740–742.
[41] R.K. Joshi, P. Carbone, F.C. Wang, V.G. Kravets, Y. Su, I.V. Grigorieva, H.A. Wu, A.K. Geim, R.R. Nair, Precise and ultrafast molecular sieving through graphene oxide membranes, Science 343 (2014) 752–754.
[42] A. Akbari, P. Sheath, S.T. Martin, D.B. Shinde, M. Shaibani, P.C. Banerjee, R. Tkacz, D. Bhattacharyya, M. Majumder, Large-area graphene-based nanofiltration membranes by shear alignment of discotic nematic liquid crystals of graphene oxide, Nat. Commun. 7 (2016) 10891.

[43] M.E.A. Ali, L. Wang, X. Wang, X. Feng, Thin film composite membranes embedded with graphene oxide for water desalination, Desalination 386 (2016) 67–76.
[44] B. Chen, H. Jiang, X. Liu, X. Hu, Molecular Insight into water desalination across multilayer graphene oxide membranes, ACS Appl. Mater. Interfaces 9 (27) (2017) 22826–22836.
[45] M. Hu, B. Mi, Enabling graphene oxide nanosheets as water separation membranes, Environ. Sci. Technol. 47 (8) (2013) 3715–3723.
[46] B. Liang, W. Zhan, G. Qi, S. Lin, Q. Nan, Y. Liu, B. Cao, K. Pan, High performance graphene oxide/polyacrylonitrile composite pervaporation membranes for desalination applications, J. Mater. Chem. A 3 (9) (2015) 5140–5147.
[47] A. Nicolai, B.G. Sumpter, V. Meunier, Tunable water desalination across graphene oxide framework membranes, Phys. Chem. Chem. Phys. 16 (18) (2014) 8646–8654.
[48] M. Safarpour, A. Khataee, V. Vatanpour, Thin film nanocomposite reverse osmosis membrane modified by reduced graphene oxide/TiO 2 with improved desalination performance, J. Membr. Sci. 489 (2015) 43–54.
[49] J. Wang, P. Zhang, B. Liang, Y. Liu, T. Xu, L. Wang, B. Cao, K. Pan, Graphene oxide as an effective barrier on a porous nanofibrous membrane for water treatment, ACS Appl. Mater. Interfaces 8 (9) (2016) 6211–6218.
[50] K. Xu, B. Feng, C. Zhou, A. Huang, Synthesis of highly stable graphene oxide membranes on polydopamine functionalized supports for seawater desalination, Chem. Eng. Sci. 146 (2016) 159–165.
[51] Y. Yuan, X. Gao, Y. Wei, X. Wang, J. Wang, Y. Zhang, C. Gao, Enhanced desalination performance of carboxyl functionalized graphene oxide nanofiltration membranes, Desalination 405 (2017) 29–39.
[52] L.D. Wang, M.S.H. Boutilier, P.R. Kidambi, D. Jang, N.G. Hadjiconstantinou, R. Karnik, Fundamental transport mechanisms, fabrication and potential applications of nanoporous atomically thin membranes, Nature Nano 12 (2017) 509–522.
[53] S. Zhuang, L. Zhou, W. Xu, N. Xu, X. Hu, X. Li, G. Lv, Q. Zheng, S. Zhu, Z. Wang, J. Zhu, Tuning transpiration by interfacial solar absorber-leaf engineering, Adv. Sci. 5 (2) (2018) 1700497.
[54] N. Xu, X. Hu, W. Xu, X. Li, L. Zhou, S. Zhu, J. Zhu, Mushrooms as efficient solar steam-generation devices, Adv. Mater. 29 (28) (2017) 1606762.
[55] W. Xu, X. Hu, S. Zhuang, Y. Wang, X. Li, L. Zhou, S. Zhu, J. Zhu, Flexible and salt resistant janus absorbers by electrospinning for stable and efficient solar desalination, Adv. Energy Mater. 8 (14) (2018) 1702884.